INDONESIAN JOURNAL ON GEOSCIENCE
Geological Agency
Ministry of Energy and Mineral Resources

Journal homepage: http://ijog.geologi.esdm.go.id
ISSN 2355-9314, e-ISSN 2355-9306

Pacific-Gondwana Permo-Triassic Orogenic Belt with Lesser Overprinted Cenozoic Deformation, Eastern Bird Head Peninsula, West Papua, Indonesia

Sukahar Eka Adi Saputra[1,2] and Christopher L. Fergusson[1]

[1]School of Earth, Atmospheric, and Life Sciences, University of Wollongong, NSW, 2522, Australia
[2]Centre for Geological Survey-Geological Agency of Indonesia, Bandung, 40122, Indonesia

Corresponding author: cferguss@uow.edu.au
Manuscript received: September, 17, 2022; revised: October, 8, 2022;
approved: November, 24, 2022; available online: March, 10, 2023

Abstract - The Paleozoic to Early Mesozoic Pacific-facing active margin of East Gondwana has been shown to extend into the Kemum Block of northern Bird Head Peninsula (western New Guinea), and was associated with Mid Paleozoic orogenic deformation and Devonian to Triassic silicic magmatism and foreland basin deposition. In the Mawi Bay area of the eastern Bird Head Peninsula, the (?) Permian Mawi Complex is a multiply-deformed unit with a pre-Late Triassic D_1 deformation formed in an Andean back-arc setting associated with active margin tectonism. The D_1 deformation is characterized by recumbent, isoclinal to tight, north-northeast facing folds with an axial planar S_1 cleavage formed at a low metamorphic grade, and predated the unconformably overlying Upper Triassic - Middle Jurassic Tipuma Formation. South of the Mawi Complex, the Mesozoic-Paleogene succession of the northern Lengguru Fold Belt is affected by north-northwest trending folds, cleavage, and most of the succession dips moderately to gently to the west-southwest. This deformation is reflected in the underlying Mawi Complex by northwest-trending D_2 structures that have folded the D_1 folds, and have steeply inclined open to gentle folds, some polyclinal folds, and fault-related folds. The structures in the northern Lengguru Fold Belt may have influenced The Pliocene to Quaternary Central Bird Head Monocline associated with the Kemum Block uplifting in the northern Bird Head Peninsula.

Keywords: Central Bird Head Monocline, East Gondwana, Lengguru Fold Belt, Mawi Complex, multiply-deformed, structure

How to cite this article:
Saputra, S.E.A. and Fergusson, C.L., 2023. Pacific-Gondwana Permo-Triassic Orogenic Belt with Lesser Overprinted Cenozoic Deformation, Eastern Bird Head Peninsula, West Papua, Indonesia. *Indonesian Journal on Geoscience*, 10 (2), p.119-138. DOI: 10.17014/ijog.10.2.119-138

Introduction

Background

Gondwana in the Paleozoic to Early Mesozoic had an active margin facing the Paleo-Pacific Ocean as shown by the orogenic belts developed along South America, Antarctica, and Australia including islands in the Southwest Pacific (*e.g.* New Zealand and New Guinea, Figure 1; Cawood, 2005; Torsvik and Cocks, 2013). In the northern Bird Head Peninsula of northwestern New Guinea (eastern Indonesia), the Gondwana orogenic belt is exposed in the Kemum Block (Figure 2), a Late Cenozoic uplift bounded on its southern side by the Central Bird Head Monocline (Figure 3; Pieters *et al.*, 1985; Decker *et al.*, 2009; Saputra, 2021). The Cenozoic uplift also extends to the Cendrawasih Bay (Kusnida *et al.*, 2023). The Kemum Block has a core of Silurian to Devonian, deformed, low- to high-grade metamorphosed,

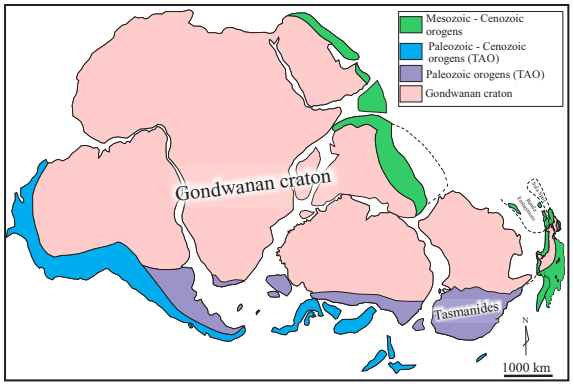

Figure 1. Gondwana showing the Terra Australis Orogen (TAO) of Cawood (2005) including more detail on New Guinea (modified from Davies, 2012).

quartz-rich turbidites, and is intruded by Devonian to Triassic granitic rocks (Pieters *et al.*, 1985; Jost *et al.*, 2018, 2021). In the Mawi Bay area, a distinct part of the southeastern Kemum Block, there are exposures of the (?) Permian multiply deformed Mawi Complex consisting of mudstones and interbedded quartz-lithic sandstones and the overlying less-deformed Triassic to Cenozoic clastic and carbonate succession (Figure 3; Pieters *et al.*, 1985; Atmawinata *et al.*, 1989). Aims of the study are to: (1) describe and interpret the structure of the Mawi Complex and the overlying Mesozoic-Cenozoic succession along recently upgraded road cuttings of the Manokwari-Bintuni Road in the Mawi Bay area south of Ransiki (Figures 1 and 2); (2) compare the setting of the Mawi Complex to the Paleozoic to lower Mesozoic Tasman Orogenic Belt (Tasmanides) of eastern Australia (Henderson *et al.*, 2013; Jessop *et al.*, 2019); and (3) outline overprinting by deformation associated with the northern extremity of the Lengguru Fold Belt (Figure 3; Dow and Sukamto, 1984; Decker *et al.*, 2009).

Regional Setting

The Mawi Bay area occurs near the junction of the southeastern Kemum Block, Central Bird Head Monocline and northern termination of the Lengguru Fold Belt, as well as ~10 km west of the seaward extension of Ransiki Fault that is the boundary to the mountainous Arfak Block (Figure 3). The Kemum Block is distinctive in New Guinea as it contains a large region underlain by Silurian-Devonian turbidites (Kemum Formation) that are characterized by isoclinal folding and foliation development indicative of

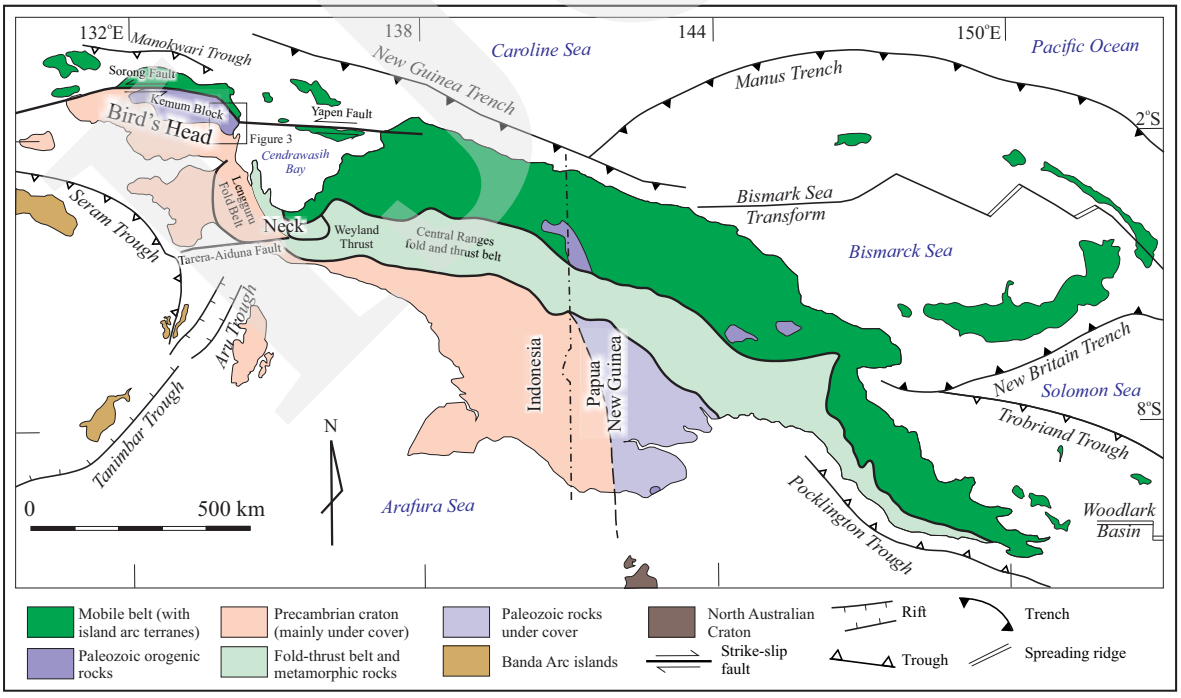

Figure 2. Simplified map of the geological elements of New Guinea (modified and reinterpreted from Davies, 2012).

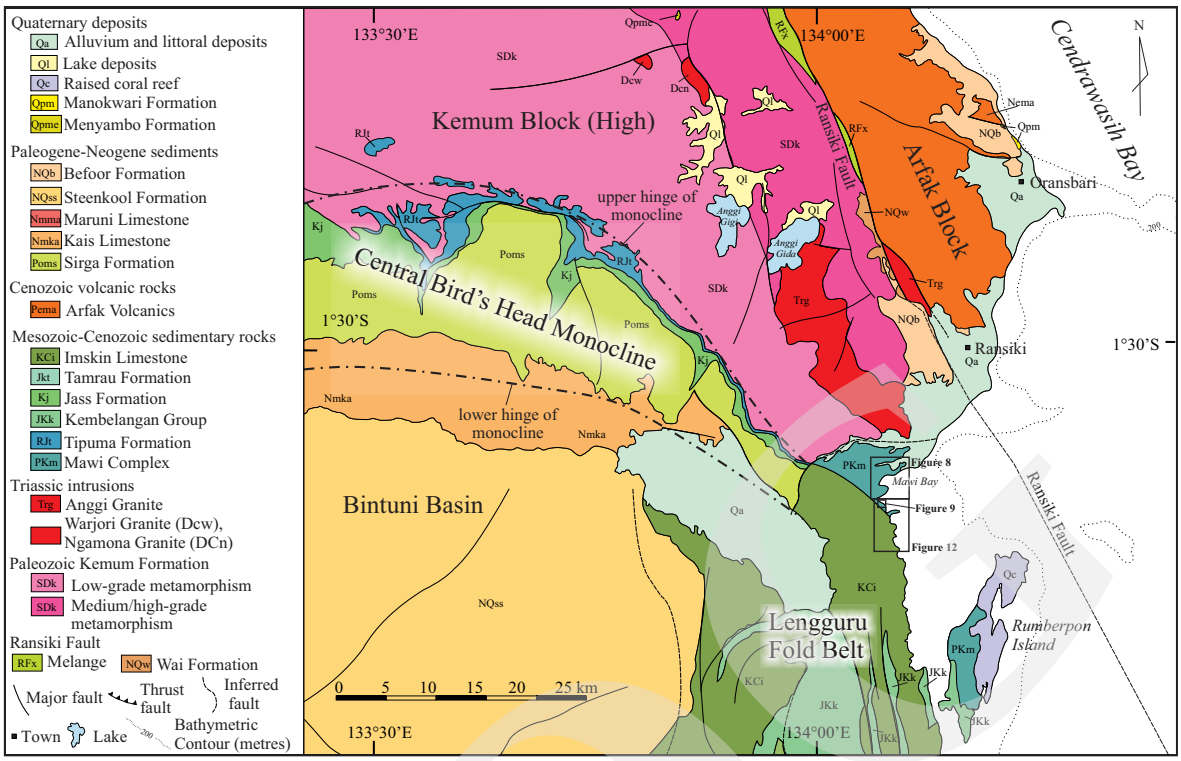

Figure 3. Geological map of part of the eastern Bird Head Peninsula, western New Guinea. Reinterpreted from the 1:250,000 scale geological maps of Atmawinata *et al.* (1989) and Ratman *et al.* (1989). Triassic ages of intrusions from Jost *et al.* (2018). See Figure 2 for location.

convergent margin orogenic processes (Pieters *et al.*, 1985; Jost *et al.*, 2021). No equivalents of the Kemum Formation have been recognized elsewhere in New Guinea, but are widespread in the Paleozoic orogenic belts (The Tasmanides) of eastern Australia *(e.g.* Rosenbaum, 2018). Granitic rocks in the Kemum Block have U-Pb zircon ages of Devonian to Triassic and have been interpreted as having formed in the roots of a magmatic arc that also produced a moderate to high-grade metamorphism in the eastern Kemum Formation (Jost *et al.*, 2018, 2021). The magmatic arc is documented in Papua New Guinea for the Triassic (Crowhurst *et al.*, 2004), and is widely developed in the Tasmanides for the Silurian to the Triassic (Henderson *et al.*, 2013; Jell, 2013; Rosenbaum, 2018; Jessop *et al.*, 2019). Along the southern margin of Kemum Block, there is the south dipping Tipuma Formation, Kembelangan Group, and overlying units that form the Central Bird Head Monocline (Figure 3; Atmawinata *et al.*, 1989). The Tipuma Formation formed in a foreland setting related to a Triassic to Middle Jurassic south-dipping subduction zone and magmatic arc along the northern margin of Gondwana and a continuation of the Permian-Triassic magmatic arc in eastern Australia and Papua New Guinea (Crowhurst *et al.*, 2004; Gunawan *et al.*, 2012, 2014; Jessop *et al.*, 2019). The Late Jurassic to Cenozoic succession postdating the Tipuma Formation formed in a rifted margin setting (Decker *et al.*, 2009). The Central Bird Head Monocline involves the Triassic to Pliocene sedimentary succession and must be no older than Pliocene (Atmawinata *et al.*, 1989). Caves and underground drainages in the lower to Mid Miocene Kais limestone on the dipping central limb of the monocline are of Pleistocene age suggesting a similar age of uplift (Thery *et al.*, 1999). Formation of the monocline was associated with the Late Cenozoic uplift of Kemum Block (Decker *et al.*, 2009). At the east of the Kemum Block, there is Arfak Block containing a Mid Cenozoic island-arc succession,

most likely accreted in the latest Oligocene and subsequently offset by strike-slip faulting along the Ransiki Fault (Webb *et al.*, 2020).

The Lengguru Fold Belt located in the south of Mawi Bay, is an arcuate belt of folds and associated thrust faults extending southwards to the Tarera-Aiduna Fault (Figure 2; Dow and Sukamto, 1984; Bailly *et al.*, 2009). The Lengguru Fold Belt has a Permian to Cenozoic clastic and carbonate succession affected by north-trending folds in the north that gradually curve southwards to a southeast and a near east-west trend adjacent to the Tarera-Aiduna Fault. The folds are associated with east to northeast-dipping thrusts, which at depth link into a near flat-lying décollement (Dow and Sukamto, 1984; Bailly *et al.*, 2009). Southwest convergence from not earlier than Late Miocene and into Pliocene (5-3 Ma) has formed the Lengguru Fold Belt (White *et al.*, 2019). This Fold Belt is situated at the western end of the Neogene foreland fold and thrust belts that form the mountainous spine of New Guinea, between the Precambrian Craton in the south and the mobile belt, including accreted island arcs in the north (Figure 2; Visser and Hermes, 1962; Dow and Sukamto, 1984; Cloos *et al.*, 2005; Bailly *et al.*, 2009; Davies, 2012; Baldwin *et al.*, 2012).

On the northeastern side of the Lengguru Fold Belt there is the rugged Wandamen Peninsula containing medium to high grade metamorphic rocks formed in multiple episodes of Neogene shortening and extension (François *et al.*, 2016; White *et al.*, 2019). Most authors favour development of the Wandamen Peninsula as a metamorphic core complex at least in part (Charlton, 2010), and White *et al.* (2019) recorded an early phase of extension at ~6 to 5 Ma based on U–Pb zircon ages followed by several deformational episodes involving alternating compression and extension.

The Mawi Bay opens eastwards into the much larger Cendrawasih Bay which is a large triangular feature 175 km long in a north-south direction and 240 km across in the north, south of Yapen Island (Figure 2). Compressional structures and associated thick sedimentary successions have been documented by seismic profiles in Cendrawasih Bay; unfortunately, these lack deep well control so that uncertainties remain about the timing of events (Decker *et al.*, 2009; Sapiie *et al.*, 2010; Babault *et al.*, 2018). Charlton (2010) interpreted Cendrawasih Bay as having formed a spenochasm due to Pliocene-Recent anticlockwise rotation of the Bird Head Peninsula driven by Pacific Plate motion and tightening the Banda Arcs in the process. Charlton (2010) considered that the thick sedimentary succession, especially in the eastern part of the bay and the adjacent Waipoga Trough, was caused by this rotation and associated with deposition of a thick Pliocene extensional succession. Alternatively, Babault *et al.* (2018) considered Cendrawasih Bay to have formed by extension in The Mid to Late Miocene (12-10 Ma) in contrast to the much younger timing advocated by Charlton (2000, 2010). As pointed out by Sapiie *et al.* (2010) the origin and basement of Cendrawasih Bay are a major problem in understanding the tectonics of New Guinea.

Stratigraphy

The Mawi Complex was mapped between the overlying Mesozoic Kembelangan Group and the Kemum Formation (Figure 3) by Pieters *et al.* (1985) and Atmawinata *et al.* (1989), but our new mapping within the enlarged road cuttings along the Manokwari-Bintuni Road has enabled further subdivision into the Mawi Complex proper and the Tipuma Formation. The numbers such as "18SE-100" in the figure captions are outcrop numbers from the field mapping, followed by the latitude and longitude of the outcrops.

The Mawi Complex consists of very low grade metamorphic, gray to black claystone and interbedded thin to thick micaceous quartz-lithic sandstones (Figure 4a; Pieters *et al.*, 1985; Atmawinata *et al.*, 1989). Graded beds have been recognized in some exposures allowing determination of younging, but most outcrops lack of sedimentary structures apart from bedding and plane lamination. The Mawi Complex is strongly deformed, lack of discernible fossils and has been correlated with the Permian Aiduna Formation

Figure 4. Rock types of the Mawi Bay area. (a) Mawi Complex, interbedded black mudstone and thin fine sandstone beds, southern limb of an antiform, sample 18SE-18. (b) Contact (white dashed line) between the Mawi Complex and the overlying Tipuma Formation, on the north side of the big road cutting (Gunung Botak) as seen at Figure c. (c) The lowest part of the Kembelangan Group overlying the Tipuma Formation in the big road cutting at Gunung Botak. (d) Interbedded red mudstone and quartz sandstone overlying conglomerate of the Tipuma Formation. (e) Gently dipping Imskin limestone to the south-southwest with steeply east-dipping calcite veins (parallel to white dashed line), sample 18SE-20.

south of the Weyland Thrust in the Bird Neck and the Aifam Group of the western Bird Head Peninsula (Visser and Hermes, 1962; Pigram and Sukanta, 1982; Sukanta and Pigram, 1989; Irawan *et al.*, 2014; Irawan, 2015). The relationship of the Mawi Complex to the Kemum Formation is not established, although it is shown on the Ransiki 1:250,000 geological map as a possible faulted contact (Atmawinata *et al.*, 1989).

The Tipuma Formation is exposed along the Central Bird Head Monocline and in the Mawi Bay area around Gunung Botak (Figures 4b and c). It mainly consists of reddish mudstone, siltstone, sandstone, and conglomerate (Figures 4b-d; Pieters *et al.*, 1985). Abundant detrital zircons with U-Pb ages of 280-205 Ma have been obtained from samples in the Tipuma Formation located on the upper part of the Central Bird Head Monocline 45 km northwest of the Mawi Bay area, and indicate deposition during Upper Triassic to Middle Jurassic (Gunawan *et al.*, 2012, 2014). It overlies the Mawi Complex, although the contact in the Mawi Bay area shows widespread brittle deformation.

The Kembelangan Group is exposed along a cuesta scarp of the Central Bird Head Monocline and in a coastal area around Mawi Bay (Figure 4c). The unit mainly consists of calcareous shale, noncalcareous shale, siltstone, sandstone, minor biocalcarenite, and conglomerate (Pieters *et al.*, 1985, 1990). Based on benthic foraminifera, belemnites, and ammonites, the unit has a Middle Jurassic to Upper Cretaceous age (Pieters *et al.*, 1985) that is broadly consistent with U-Pb detrital

zircon ages reported by Decker *et al.* (2017). It conformably overlies the Tipuma Formation at Gunung Botak (Figure 4c).

The Imskin Formation is part of the New Guinea Limestone Group (Pieters *et al.*, 1983a and b) and widely exposed in the Lengguru Fold Belt (Atmawinata *et al.*, 1989). The unit has fossiliferous calcilutite, marlstone, and minor fine calcarenite (Figure 4e). Based on planktonic foraminifera, Gold *et al.* (2017) dated the Imskin limestone as Upper Cretaceous (Campanian to Maastrichtian) to Eocene. The unit conformably overlies the Kembelangan Group south of the Mawi Bay area.

Result And Analysis

Field work was conducted in four short periods within the timeframe of January 2016 to May 2018.

Structure of the Mawi Complex

The structure of The Mawi Complex and the overlying Mesozoic to Cenozoic succession is exposed in road cuttings, many of which are intensely weathered, along The Manokwari - Bintuni Road. Structural complexity was recognized in the earlier mapping, but structural detail was not discernible due to overprinting fracturing and weathering resulting in common red iron-stained outcrops (Pieters *et al.*, 1985). Two main deformations (D_1 and D_2) have been recognized in the Mawi Complex. D_1 is associated with a slaty to spaced cleavage (S_1) in mudstones and sandstones, respectively, and axial planar to recumbent to moderately inclined folds (F_1) in bedding (Figures 5a, b, d). D_2 refers to a range of structures that have folded S_1 and associated recumbent folds, which are mainly upright, open to gentle folds but also include some polyclinal folds and folds associated with thrust faults (Figures 6 and 7).

Bedding (S_0) is divided into two domains, one in the northeast along cross-section line GH (the northeast domain), and the other along cross-section lines IJ and KL including the road cuttings around Gunung Botak (the southwest domain, Figures 8 and 9). In the northeast domain, S_0 is folded about a regional fold axis trending 5°/132°, whereas in the southwest domain, the regional fold axis is 6°/338° (Figure 10a, b). Overall, the structural trends swing from north-northwest to northwest from north to south in the Mawi Complex. These regional trends reflect the orientation of structures associated with D_2 as the F_1 folds are recumbent and thus lack of a dominant structural grain, although the trends in these domains are similar to F_1 and S_0–S_1 intersection lineation (L_1) trends (Figures 10d, e).

The D_1 deformation is characterized by the low-angle orientation of the slaty cleavage (S_1) developed in mudstones. The cleavage is defined by very fine-grained aligned muscovite (Pieters *et al.*, 1985, p. 150) consistent with very low-grade regional metamorphism. Tight to isoclinal F_1 folds (using the interlimb fold classification of Pluijm and Marshak, 2004) with axial planar S_1 have been identified at a few localities (Figure 5a), but are generally not evident in the more weathered road cuttings. Orientation of the D_1 structures is given in Figures 8, 9, and 10. S_1 has a mean orientation of 23°/009° (Figure 10c), and the calculated intersections between S_0 and S_1 for coupled measurements taken adjacent to each other are northwest-southeast trending and gently plunging (mean L_1 12°/306°; Figure 10d), whereas the mean F_1 is 1°/326° (Figure 10e). This variation is more likely a reflection of the small number of measurements (13 for F_1, 15 for L_1) rather than indicating S_1 is nonaxial planar to F_1. Axial planes of F_1 are near horizontal as expected for recumbent folds (Figure 10f). Few parasitic fold couples are exposed that can be used to indicate the sense of vergence from the overall asymmetry with "s" folds on the upright limb and "z" folds on the overturned limb. The common development of S_0 and S_1 either subparallel or at a low-angle to each other is consistent with the isoclinal nature of F_1, and indicates most of the exposed bedding planes that are on the limbs of folds.

In cross-section GH (Figures 8 and 11) drawn perpendicular to the regional fold axis determined

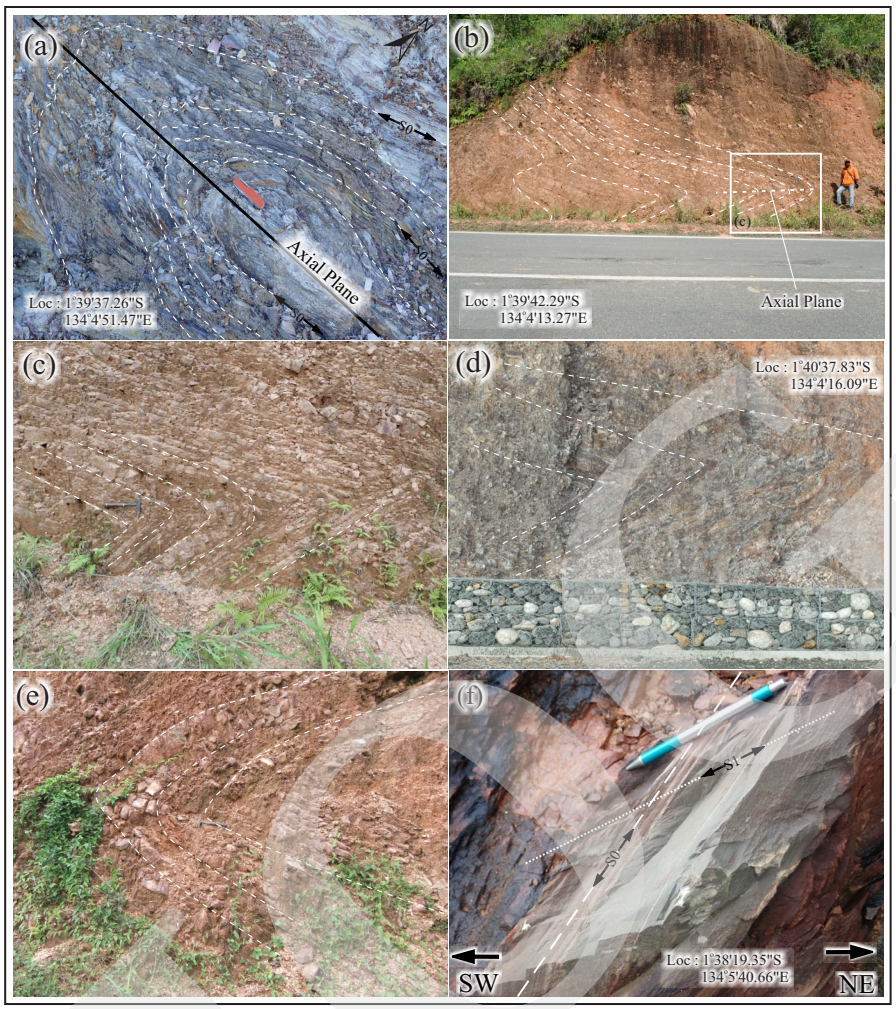

Figure 5. F_1 folds in the Mawi Complex. (a) Moderately inclined isoclinal F_1 fold, Fen knife for scale (~10 cm long). White dashed lines outline bedding (S_0). (b) Recumbent F_1 fold , photograph looking east, sample 18SE-142. (c) Enlarged from (b). (d) Recumbent F_1 fold Stone wall ~1.2 m high, photograph looking south, sample 18SE-47. (e) Recumbent F_1 fold. Photograph looking east. Geological hammer (33 cm long) for scale. (f) Bedding-cleavage relationships with S_1 dipping moderately to the southwest and more steeply dipping bedding. This indicates the exposure is on the lower limb of a F_1 antiform located to the southwest. Photograph looking northwest. Pen (15 cm long) for scale, sample 18SE-124.

for the northeast domain, most S_0-S_1 vergence is towards the north, *i.e.* the upper limb of an isoclinal hinge to the northeast. This is consistent with identification of some "z" shaped parasitic fold couples. One determination of stratigraphic younging from graded beds indicates that this fold is a northeast-facing anticline. S_0-S_1 vergence determined from one outcrop further to the northeast indicates that vergence is in the opposite direction, *i.e.* the anticline hinge has been crossed, and it is here part of the lower limb (Figure 5f).

In the southwest domain two cross-sections IJ and KL have been drawn perpendicular to the regional fold axis (Figure 11). In the northwest cross-section IJ, vergence has only been determined from two "z" shaped parasitic fold couples that indicate the rocks are still part of the upper limb of a north-facing anticline as was determined for much of cross-section line GH. Graded bedding has been recognized at several localities along this cross-section line and are all upright consistent with these rocks being part of the upper, upright limb of a map-scale recumbent fold. In the southwest cross-section KL (Figure 11), four changes of vergence occur indicating that the overturned limb of a north-facing anticline is developed between two upper limbs. This is based on both the asymmetry of parasitic fold couples

Figure 6. F_2 folds in the Mawi Complex. (a) Photograph of F_2 fold with axial plane steeply dipping to east 60°/082°. Dashed white lines show bedding (S_0). Geological hammer for scale (33 cm long) in circle, sample 18SE-128. (b) Photograph of open polyclinal folds. Dashed black lines outline bedding, sample 17 SE-79. (c) Gentle upright F_2 folds (dashed white lines show bedding) with steeply west-dipping limb on the left; highly weathered cutting with common staining by Fe_2O cutting is ~7m long. Sample 18SE-15. (d) Upright southeast plunging F_2 synform. Photograph looking northwest. Pen for scale (15 cm long), 18SE-123. (e) Upright rounded F_2 antiform, photograph looking northwest. Hinge is ~1.5 m across, 18SE-126.

and the changes in the S_0-S_1 vergence senses from one limb to the other. The overturned limb in the eastern part of this cross-section contains the most well exposed S_0-S_1 relationships along the whole traverse across the Mawi Complex.

The presence of recumbent folds developed over a distance of 5 km in a northeast direction implies considerable shortening has affected the Mawi Complex in this deformation. The northward-facing recumbent folds and short overturned limbs suggest northeast tectonic transport.

The D_2 deformation has formed mainly upright to steeply inclined, northwest-southeast trending folds with open-gentle interlimb angles that fold the limbs of the F_1 recumbent folds. This deformation is responsible for locally steep dips and more common moderate dips developed in parts of the Mawi Complex (Figures 8 and

Figure 7. Late, steeply to moderately inclined folds in bedding (outlined by white dashed lines) associated with moderately south-dipping thrust faults (shown by white continous lines) indicating tectonic transport to the north (18SE-48, 1°40'38.34"S, 134°4'14.81"E). Photograph looking west.

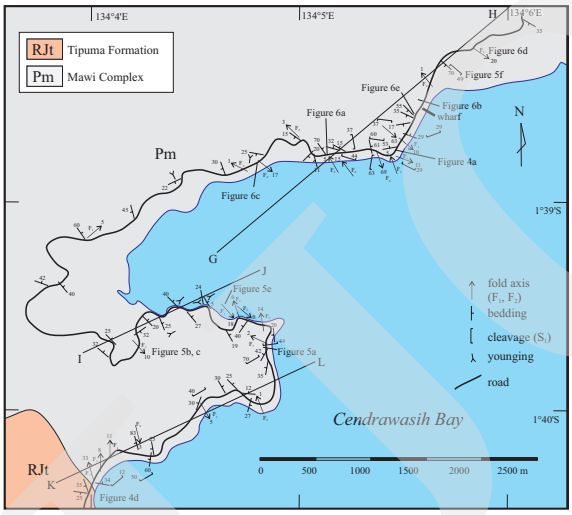

Figure 8. Local geological map of the northeastern part of Mawi Bay area showing structural data in the Mawi Complex collected during this study. Fold axes are labelled F_1 and F_2. See Figure 3 for location. Approximate locations of photographs (Figures 4a, d, 5a-c, e, 6a-e) shown.

9). F_2 have a mean orientation of 4°/134° and axial planes dip steeply to the northeast (mean 76°/051°; Figure 10g, h). F_2 are "stumpy" folds, *i.e.* they have low amplitude to wavelength ratios (Figure 6), and thus have a relatively low level of shortening. Additionally, some disharmonic, polyclinal folds occur and have low-dipping axial planes in addition to folds with steeper axial planes (Figures 6b, d, e).

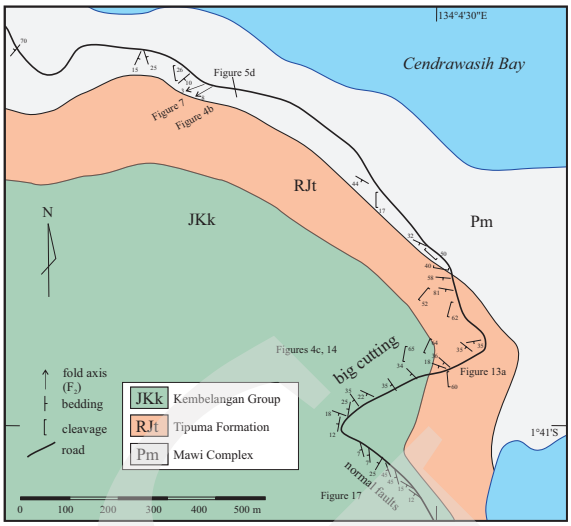

Figure 9. Detailed geological map of Gunung Botak Point area showing structural data collected during this study. See Figure 3 for location. Approximate locations of photographs (Figures 4b, c, 5c, 7, 13a and 17) shown.

In one exposure adjacent to the faulted contact with the overlying Tipuma Formation, small F_2 z-fold couples are developed with short steeper forelimbs and associated with south-dipping thrusts (Figure 7). They are interpreted as small fault-propagation folds related to north-directed thrusting. On the map-scale, F_2 have generally very high interlimb angles resulting in the low amplitude, steeply inclined folds evident in cross-sections (Figure 11).

Structure of the Tipuma Formation, Kembelangan Group, and Imskin Limestone

The Manokwari-Bintuni Road follows the coastline south of Mawi Bay and obliquely crosses the Tipuma Formation, Kembelangan Group, and Imskin limestone (Figures 9 and 12). A number of structural features are evident at outcrop scale in these rocks and include spaced cleavage (S), an intersection lineation between bedding and cleavage (L), upright folds, calcite veins, and joints (Figure 13). Outcrops in the cuttings at Gunung Botak exhibit strike-slip faults (Figure 14).

Bedding defines a regional fold axis plunging 3°/329° (Figure 15a), but the strike of bedding ranges from nearly east-west to almost north-south. In the basal Kembelangan Group and Tipu-

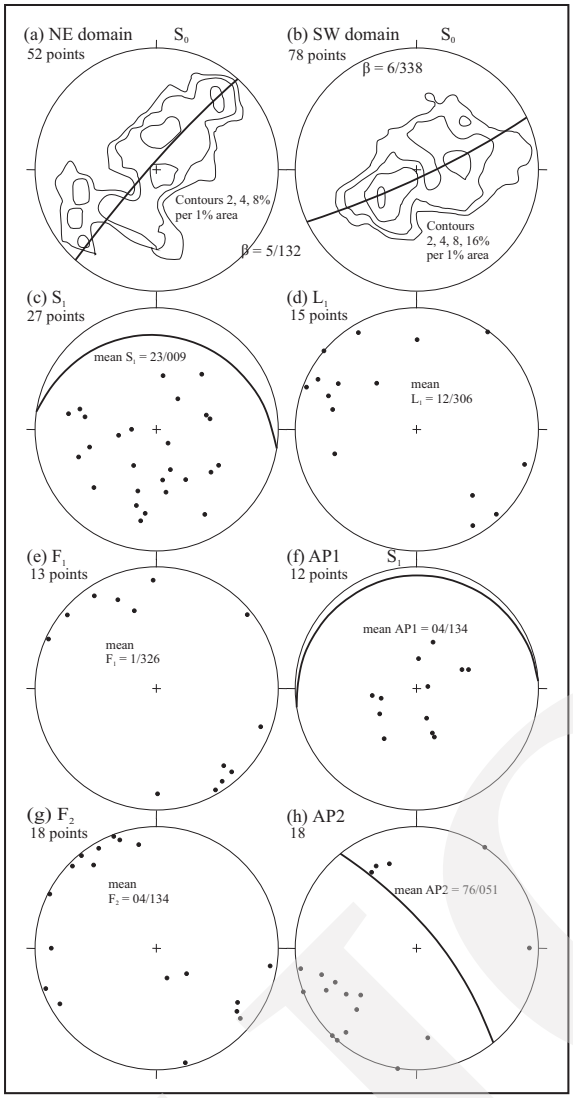

Figure 10. Equal area stereographic projections (lower hemisphere) showing structural data from the Mawi Complex in the Mawi Bay area. (a) Bedding in the northeastern domain. (b) Bedding in the southwestern domain. (c) S_1 cleavage. (d) Bedding-cleavage intersections (L_1) from coupled measurements. (e) F_1 fold axes. (f) Axial planes of F_1 folds. (g) F_2 fold axes. (h) Axial planes of F_2 folds.

ma Formation, the units dip more consistently at ~30°SW (Figures 9 and 12). The succession is dipping homoclinally to the west-southwest with common local variations (Figures 12 and 15). Some limited dips to the east occur due to a local upright, open, anticline, and syncline pair in the upper part of the Kembelangan Group (Figures 12 and 16, cross-section CD).

The spaced cleavage (S) developing in mudstones and calcareous mudstones, spaces up to several centimetres and is typically a rough,

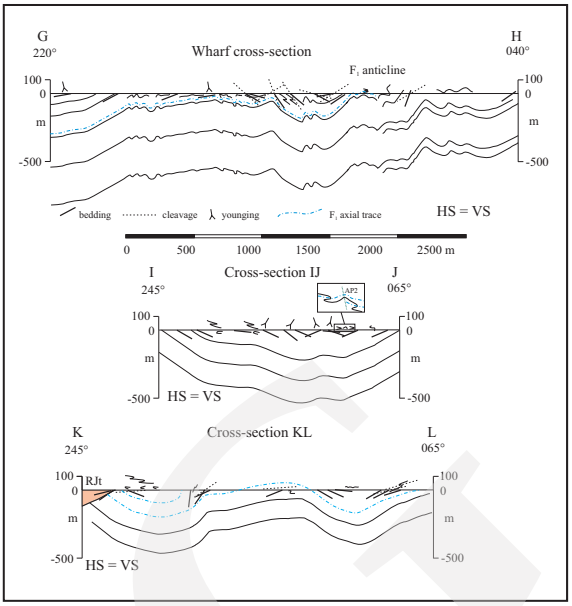

Figure 11. Cross-sections GH, IJ, and KL across the northeastern domain of the Mawi Complex. See Figure 8 for location. AP2, axial plane 2 (D_2 deformation). RJt, Triassic-Jurassic Tipuma Formation.

irregular, but overall planar structure (Figure 13). On average, it is dipping steeply to the east (72°/081°), but has a large variation in strike (300° to 020°; Figure 15b). The cleavage is axial planar to the local syncline-anticline pair. A well-developed intersection lineation between bedding and the cleavage is present on bedding planes, and plunges gently both to the north-northwest and south–southeast at an average of 5°/165° (Figure 15c) consistent with the gentle plunge of the local anticline-syncline pair.

Strike-slip and normal faults are particularly prominent in the big cutting at Gunung Botak and in the next cutting to the south respectively (Figures 9, 14, and 17). In the big cutting, numerous mainly steeply dipping faults are exposed with a common north-northeast strike (Figures 14 and 15d-f). Slickenlines, both striations and quartz fibres, define slip directions which are mainly gently plunging to the north-northeast and south-southwest, indicating that the faults have mainly strike-slip offsets. The amount of offset cannot be determined, but given the uniformity of beds offset along the faults are unlikely to be more than several metres. Steps along the fault planes have been determined from eleven of the

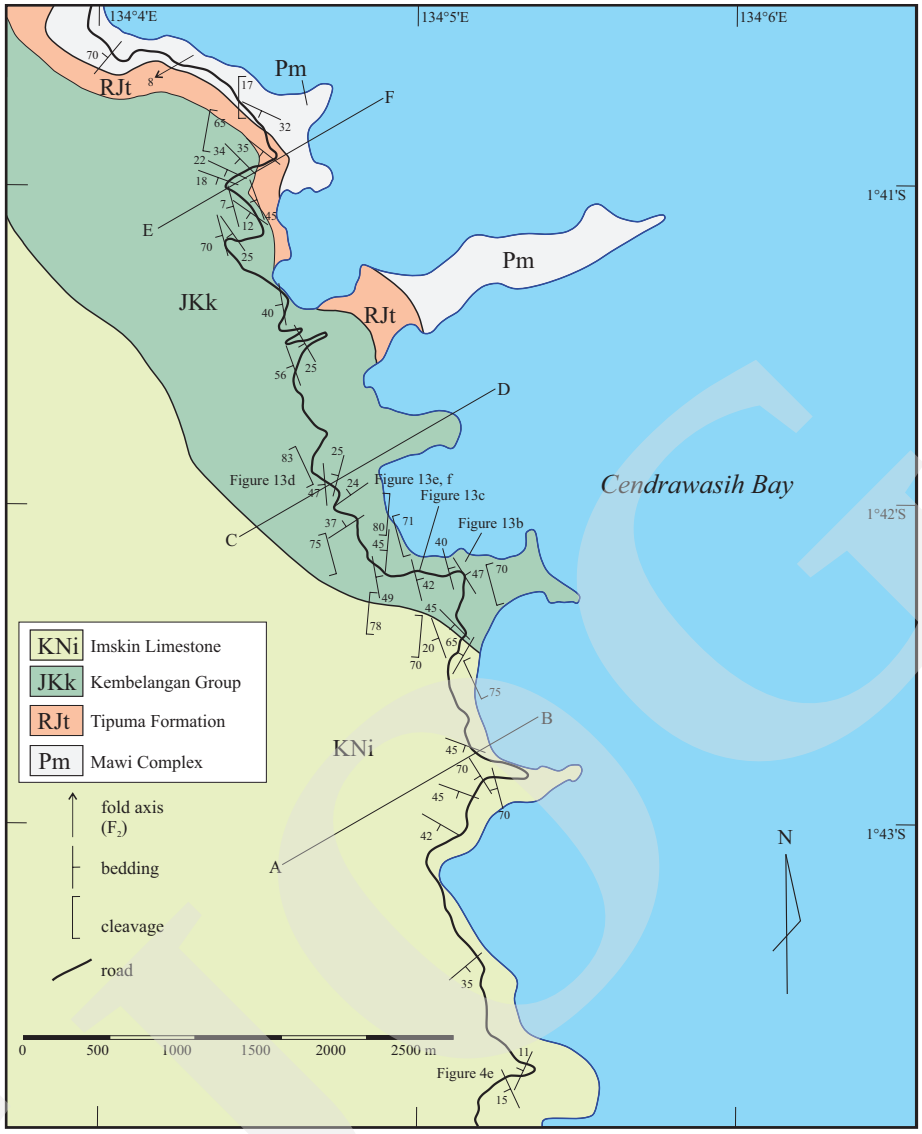

Figure 12. Local geological map of the southern part of the Mawi Bay area showing structural data collected during this study. See Figure 3 for location. Approximate locations of photographs (Figures 4f and 13b-ef) shown.

faults, and show both dextral (4) and sinistral (7) senses (Figures 15d, e). These faults are poorly constrained in age, but probably postdate the main deformation in these rocks and are potentially related to strike-slip faulting along The Ransiki Fault. Six normal faults are exposed in the southern cutting and have offsets <2 m as shown by a prominent marker bed (Figure 17). They are northeast trending, and indicate an overall northwest-southeast extension direction (Figure 15f). Their timing is poorly constrained, and it is possible that they formed closely following deposition.

Joints and thin calcite veins (<1 cm thick) are widely developed, especially in the Imskin limestone at the southern end of the traverse (Figure 4e). These are variable in orientation, but overall are steeply dipping and east-west striking (Figure 15g). They are at a high-angle to strike and presumably related to compressional stresses and fluctuating hydro-pressures that accompanied tilting, folding, and cleavage formation (see Pluijm and Marshak, 2004).

The contact between the Tipuma Formation and the underlying Mawi Complex is well exposed in road cuttings around Gunung Botak.

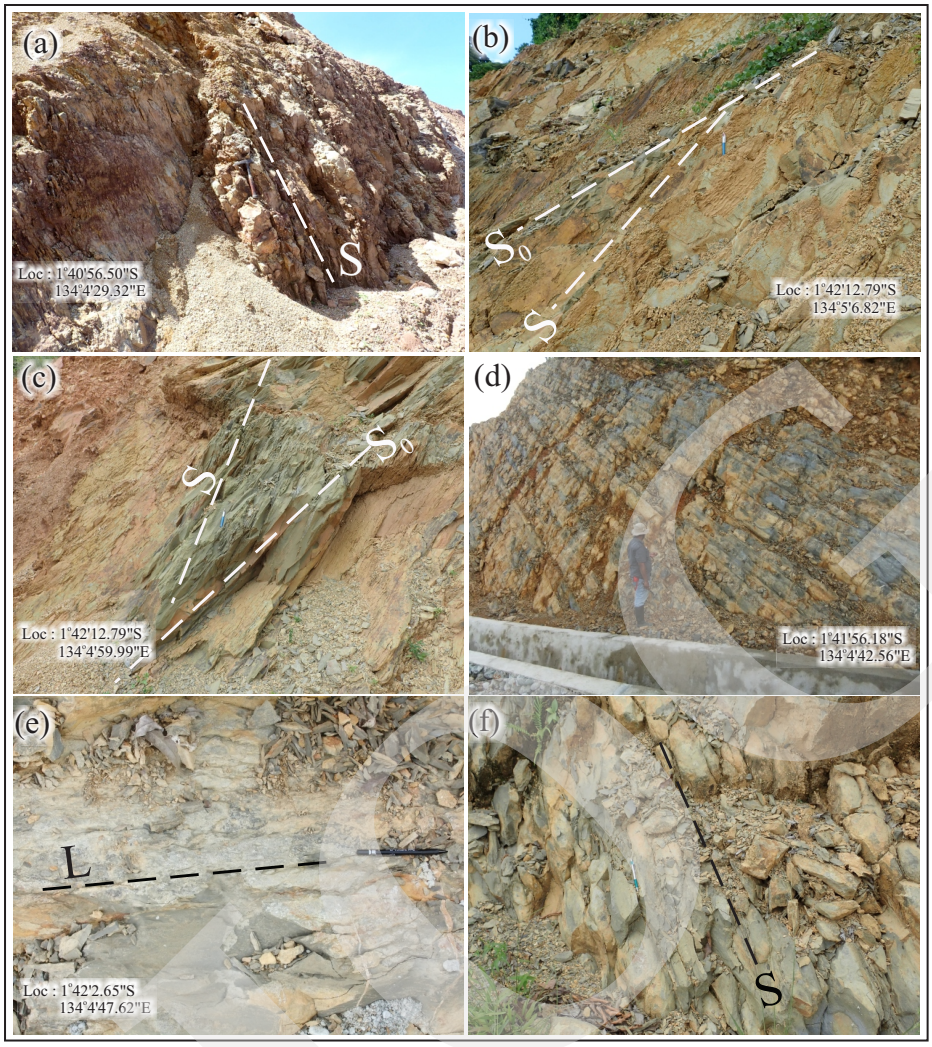

Figure 13. Bedding and cleavage within the Kembelangan Group in road cuttings south of Mawi Bay. (a) Spaced cleavage (S, dashed line) dipping steeply to the east (60°/070°) in sandstone. Photograph looking north. Geological hammer (33 cm long) for scale, sample 18SE-122. (b) Bedding (S_0, 45°/065°, dashed line) and cleavage (S, 65°/055°, dashed line). Photograph looking southeast. Pen (15 cm long) for scale, sample 18SE-99. (c) Bedding (S_0, 42°/074°) cleavage (S, 71°/074°). Photograph looking south and pen (15 cm long) for scale, sample 18SE-100. (d) Bedded limestone dipping moderately to the west-southwest. Photograph looking southwest. (e) Intersection lineation between bedding and cleavage, plunges 27°/330°. Pen (15 cm long) for scale, sample 18SE-22. (f) Spaced cleavage (S, 75°/255°, dashed line). Same location as (e). Pen (15 cm long) for scale.

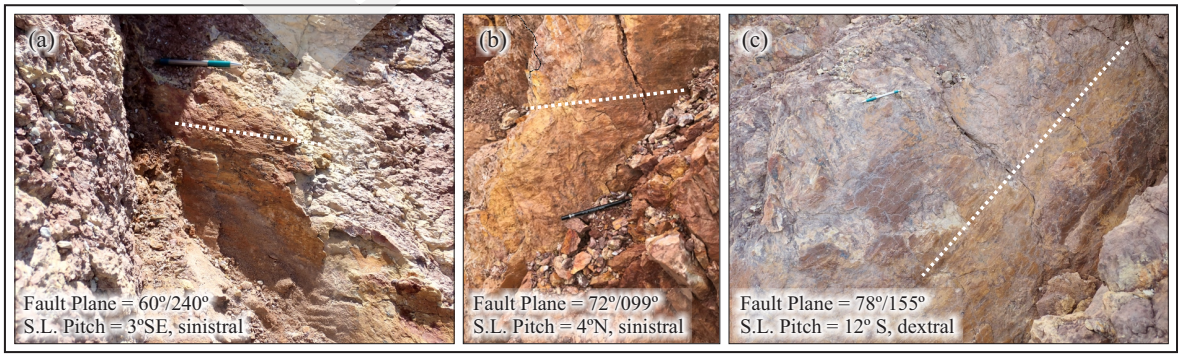

Figure 14. Strike-slip faults in the lower Kembelangan Group (Woniwogi Formation) in the big cutting (Gunung Botak, 18SE122, 1°40'56.43"S, 134°4'28.59"E). Pens 15 cm for scale. S.L., Slickenlines (dotted white lines).

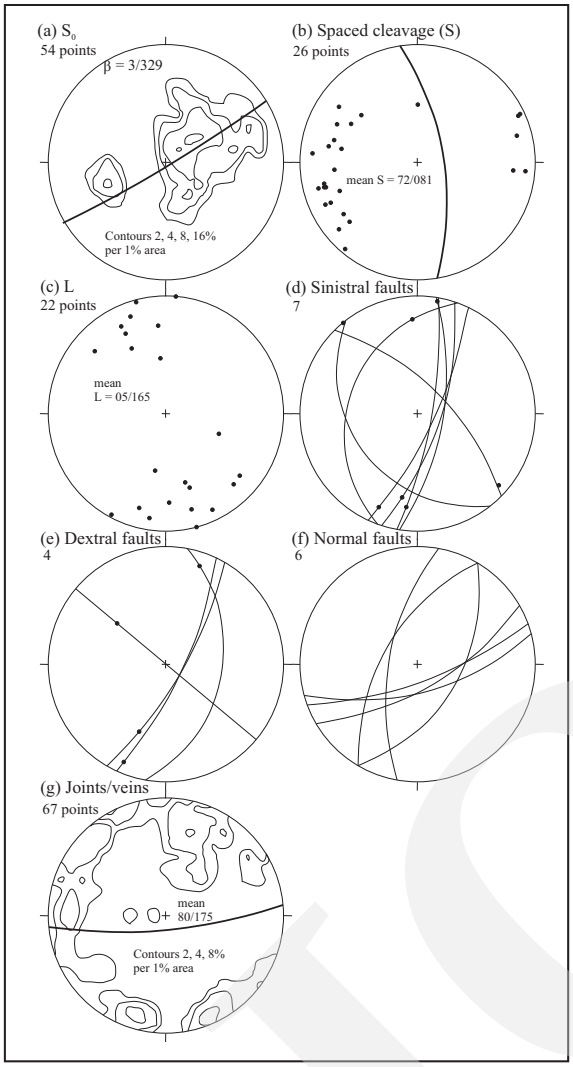

Figure 15. Equal area stereographic projections (lower hemisphere) showing structural data from the Tipuma Formation, Kembelangan Group, and Imskin limestone in the Mawi Bay area. (a) Bedding. (b) Spaced Cleavage (S). (c) Bedding-cleavage intersections (L) from coupled measurements. (d) Sinistral faults (great circles) and slickenlines (dots) from the big cutting at Gunung Botak. (e) Dextral faults (great circles) and slickenlines (dots) from the big cutting at Gunung Botak. (f) Normal Faults (great circles) from the road cutting south of the big cutting at Gunung Botak. (g) Joints and calcite veins mainly from the Imskin limestone.

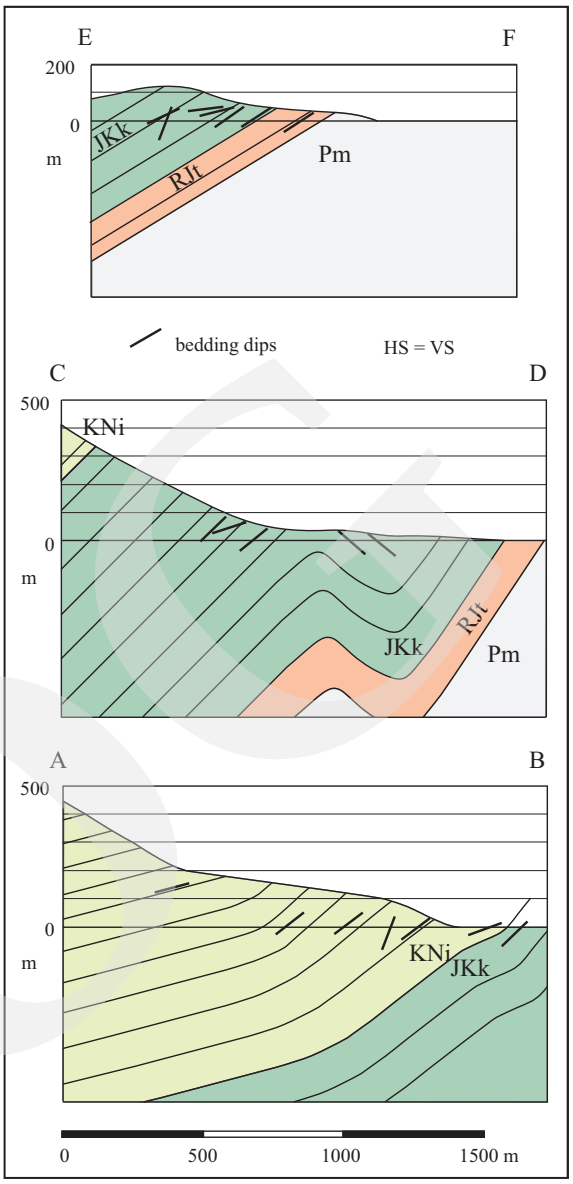

Figure 16. Cross-sections EF, CD and AB across the Mawi Complex (Pm), Tipuma Formation (RJt), Kembelangan Group (JKk), and Imskin limestone (KNi). See Figure 12 for locations.

Unfortunately, road works has resulted in widespread fracturing of the sandstones of the Tipuma Formation producing many lose blocks. The contact at map scale is a planar feature, but in detail is highly irregular with scaly shear fabrics overprinting both the Tipuma Formation and the Mawi Complex. The scaly shear fabric overprints cleavage in both units, but has no regular orientation and indicates that the contact has been a locus of faulting and dispersed brittle deformation resulting in irregular blocks (Figure 4b). Overall, the contact is subparallel to the main bedding orientation in the Tipuma Formation developed 50 m or more above the contact (Figure 9).

Discussion

The presence of black mudstones, quartz-lithic sandstones containing low-grade metamorphic

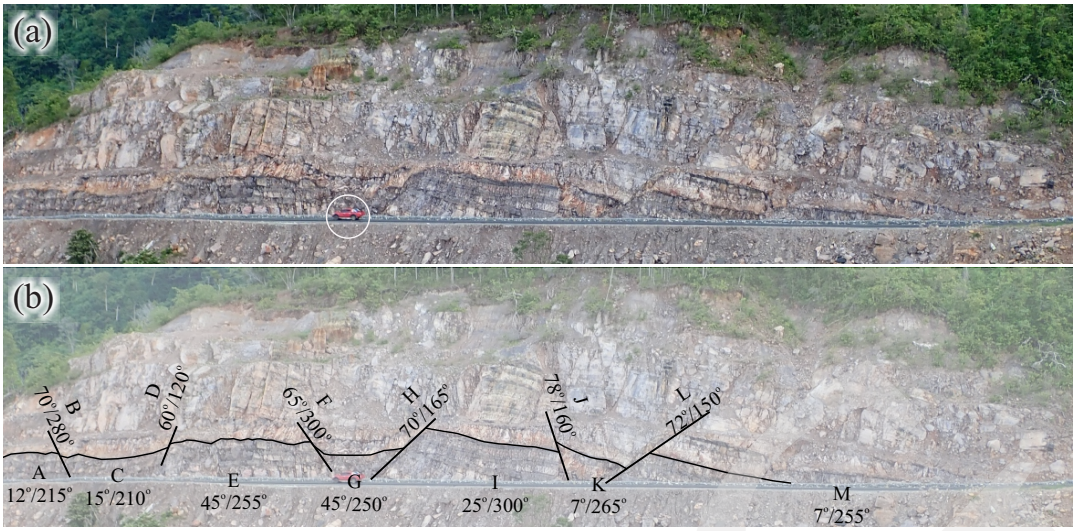

Figure 17. Normal faults developed in the Woniwogi Formation of the lower Kembelangan Group (18SE-158, 1°41'1.8"S, 134°4'25"E). Red vehicle (white circle) on road for scale.

rock fragments and detrital muscovite, and the stratigraphic position of the Mawi Complex below the Tipuma Formation, are indicative of correlation with the Permian Aiduna Formation of the Bird Neck south of the Weyland Thrust (Figure 2) and the Aifam Group of the western Bird Head Peninsula (Visser and Hermes, 1962; Irawan *et al.*, 2014; Irawan, 2015). However, the strong deformation of the Mawi Complex contrasts to the Aifam Group, which is weakly deformed in the western Bird Head Peninsula (Pigram and Sukanta, 1982; Pieters *et al.*, 1985; Sukanta and Pigram, 1989). The Aiduna Formation in the Bird Neck region south of the Weyland Thrust has been involved in The Cenozoic fold-thrust belt formed by the island-arc collision and thrusting event, but is not affected by the strong pre-Tipuma Formation D_1 deformation in the Mawi Complex (Figure 2; Panggabean and Pigram, 1989).

The setting of the Mawi Complex needs to be placed in the much broader context of the Permian to Triassic Paleo-Pacific active margin of Gondwana (Figure 18a). The overlying Tipuma Formation shows evidence of Triassic magmatic activity, and has been interpreted as forming in a foreland setting adjacent to an Andean magmatic arc trending east-west through the Bird Head Peninsula, central Papua New Guinea, and north-south trending in the Tasmanides of eastern Australia (Figure 18; Hill and Hall, 2003; Gunawan *et al.*, 2012, 2014; Webb and White, 2016). These data and interpretations are consistent with the widespread Permian-Triassic ages determined for granites across the northern Bird Head Peninsula in the Kemum Block, and interpreted as part of the active Andean margin of Gondwana (Jost *et al.*, 2018). Hill and Hall (2003) suggested that the Tasmanides, which includes a compressive continental arc in the Late Permian to Mid Triassic of the New England Orogen (Jessop *et al.*, 2019), changed trend from north-south to east-west along the northern margin of New Guinea.

The recognition of Tasmanide equivalents in the Bird Head is also consistent with the Silurian-Devonian Kemum Formation, which resembles highly deformed Silurian-Devonian quartzose turbidites of the Paleozoic Mossman Orogen of North Queensland (Henderson *et al.*, 2013). Although the Mossman Orogen is ~2000 km southeast of the Bird Head Peninsula, it has the nearest known equivalents of the Kemum Formation. In Papua New Guinea, ~1400 km east-southeast of the Bird Head Peninsula, Wyck and Williams (2002) have documented metamorphic rocks of Permian to Triassic age and Triassic intrusions (see also Crowhurst *et al.*, 2004), which are a northern continuation of the New England

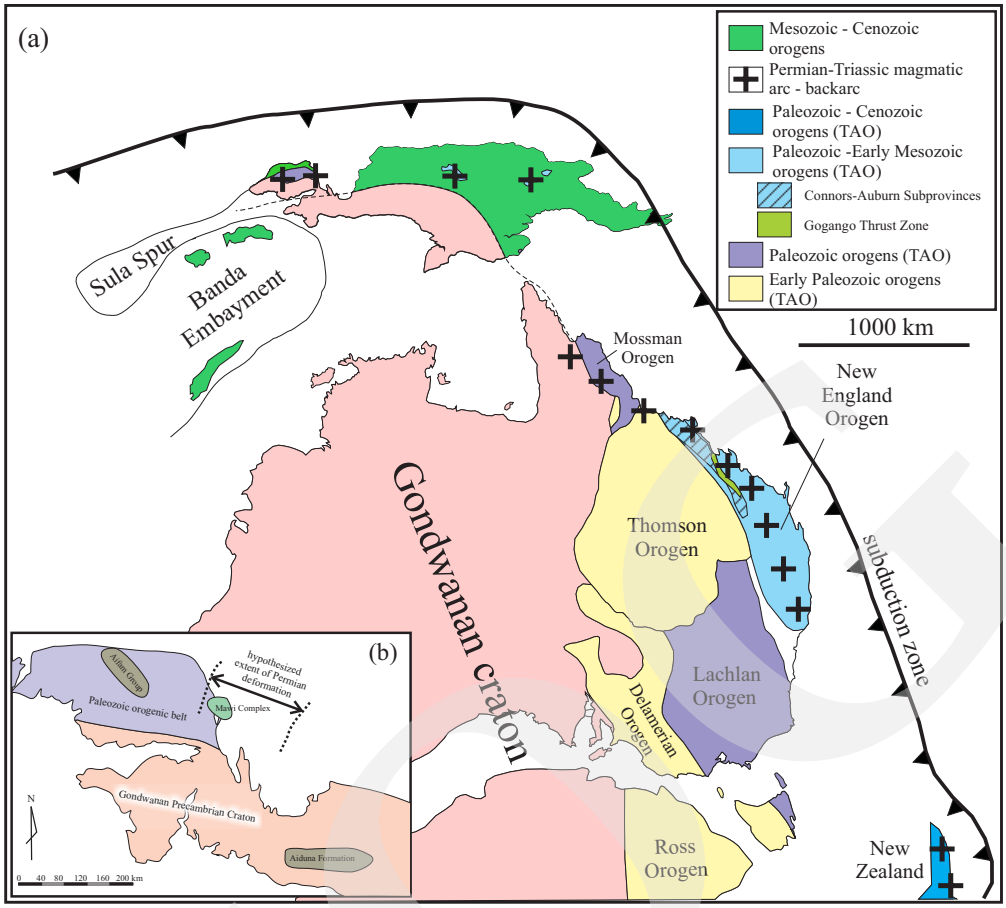

Figure 18. (a) Map of East Gondwana showing the extent of the Permian-Triassic arc-backarc superimposed on the orogenic belts of the Tasmanides of eastern Australia. (b) Map of western New Guinea showing a hypothetical distribution of the Gondwanan Precambrian Craton and the Paleozoic Orogenic Belt of the Kemum Block and the hypothesized extent of intense Permian deformation affecting the Mawi Complex based on the known exposures.

Orogen. In the New England Orogen and Mossman Orogens, Permian to Mid Triassic contractional deformation is widespread in back-arc to arc settings and known as the Hunter-Bowen Orogeny in addition to the Permian to Triassic igneous activity (Henderson *et al.*, 2013; Jell, 2013; Jessop *et al.*, 2019). The D_1 deformation of the Mawi Complex reflects localized strong inversion of a Permian sedimentary basin (Figure 18b) developed in an Andean active margin setting as interpreted for the Bird Head Peninsula by Gunawan *et al.* (2012) and Jost *et al.* (2018) for the Tipuma Formation and granitic rocks respectively. This deformation is comparable to widespread shortening of Permian successions in the New England Orogen of eastern Australia during the Hunter-Bowen Orogeny (Rosenbaum, 2018; Jessop *et al.*, 2019). For example the Gogango Thrust Zone in central Queensland contains tight folds and locally near-recumbent folds with well-developed axial plane cleavage, but dies out to the south and north into less deformed rocks of the eastern Permian-Triassic Bowen Basin (Figure 18a; Fergusson, 1991; Jell, 2013).

Northern Extent of the Lengguru Fold Belt

The Tipuma Formation, Kembelangan Group, and Imskin limestone were affected by west-southwest to east-northeast shortening producing the north-northwest trending folds, spaced cleavage, and overall west-southwest dip of these units. As is evident from the earlier mapping of the Mawi Bay area (Dow and Sukamto, 1984; Atmawinata *et al.*, 1989a, Figure 6), the structural trends of the Mesozoic-Paleogene succession gradually curve from a north-south trend west

of Rumberpon Island to a north-northwest trend south of Mawi Bay and to a northwest trend west of Mawi Bay (Figures 2 and 12). The F_2 folds in the Mawi Complex are mainly northwest-trending and within the Mawi Bay area the main structural trends, which reflect the F_2 folding, curve from a north-northwest trend in the southwest domain to a northwest trend in the northeast domain (Figure 10a and b). The D_2 deformation is considered to be a result of the overprinting Late Miocene-Pliocene deformation that affected the Mesozoic-Paleogene succession (Bailly *et al.*, 2009; White *et al.*, 2019) as shown by the complementary structural trends in both successions. Furthermore, these structural trends are traced southwards into the wider Lengguru Fold Belt, and considered to be part of this belt as shown in previous work (*e.g.* Dow and Sukamto, 1984).

Pliocene to Pleistocene Deformation Associated with Formation of the Central Bird Head Monocline

The Central Bird Head Monocline is a major structure that is associated with the uplifting of Kemum High. It is clear from previous work (Dow and Sukamto, 1984; Pieters *et al.*, 1985; Atmawinata *et al.*, 1989a) and even from topography that structural trends in the northern end of the Lengguru Fold Belt curve from a northwest to the east−west trend of the Central Bird Head Monocline (Figure 3). The transition from one to the others is seamless as is apparent from Figure 3. The Central Bird Head Monocline formed during uplift of the Kemum High potentially in Quaternary, but may extend into Pliocene (Decker *et al.*, 2009; Saputra, 2021; Saputra *et al.*, 2022). The uplift would appear to be younger than formation of the Lengguru Fold Belt, although it cannot be ruled out that they partially overlap. Given that the Central Bird Head Monocline postdates at least some deformation in the Lengguru Fold Belt, then the seamless transition between them reflects development of the location of the monocline influenced by the termination of the pre-existing structures of the northern Lengguru Fold Belt.

Conclusions

The Mawi Complex in the eastern Bird Head Peninsula is considered equivalent to the Permian Aiduna Formation exposed south of the Weyland Thrust in the Bird Neck and the Aifam Group in the western Bird Head Peninsula, but differs from both given that it was affected by strong deformation in the Permian to Early Triassic. The first deformation (D_1) in the Mawi Complex is characterized by northeast-facing, recumbent, tight to isoclinal folds containing an axial planar slaty to spaced cleavage. These structures predate deposition of the overlying Upper Triassic to Middle Jurassic Tipuma Formation indicating a Permian to Early Triassic timing for the deformation. The second deformation (D_2) in the Mawi Complex consists of gentle to close, upright to steeply inclined folds that trend north-northwest to northwest. D_2 structures have folded the D_1 structures resulting in gentle to moderate and locally steeper dips of bedding in the Mawi Complex. Other post-D_1 structures in the Mawi Complex include polyclinal folds with inclined axial planes and several small fault-propagation folds adjacent to the faulted contact with the overlying Tipuma Formation. These structures are tentatively included in the D_2 deformation. The D_2 deformation is considered related to the north -northwest trending folds and spaced cleavage developed in the overlying Mesozoic to Paleogene succession of the northern Lengguru Fold Belt. Most of this succession is dipping gently to moderately to the west-southwest.

The D_1 deformation of the Mawi Complex is unique in Permian rock units of the Bird Head Peninsula and Bird Neck, and is related to the active Gondwanan Paleo-Pacific margin of the Bird Head Peninsula in the Permian to Triassic. The Kemum Block contains Mid Paleozoic highly deformed turbidites (Kemum Formation), Devonian to Triassic granites, and Triassic igneous activity shown by detrital zircon ages and clast types in the Tipuma Formation (Gunawan *et al.*, 2012, 2014; Jost *et al.*, 2018). These features are consistent with tracing the north-south trending Tasmanides of eastern Australia into central

Papua New Guinea, and then curving westwards to continue north of the Precambrian Craton in southern New Guinea to the Kemum Block of the Bird Head Peninsula. The D_1 recumbent folds are considered equivalent to the Mid Permian to Mid Triassic Hunter-Bowen Orogeny in the New England Orogen of eastern Australia, and formed in a compressional continental margin setting.

Late Miocene to Pliocene deformation of the Lengguru Fold Belt produced the folding, cleavage, and general west-southwest dip of the Mesozoic to Paleogene succession as well as the D_2 deformation in the underlying Mawi Complex. These structures were produced during west-northwest-east-northeast shortening during the tectonic event that formed the Lengguru Fold Belt (Dow and Sukamto, 1984). The northern part of Lengguru Fold Belt appears to have influenced the east-west trending younger Central Bird Head Monocline. .

Acknowledgments

The authors thank the Indonesian Endowment Fund for Education (LPDP), the Centre for Geological Survey - Geological Agency of Indonesia, and the University of Wollongong that funded this research. The authors really appreciate the local government of West Papua Province and the Papua State University (UNIPA), Manokwari for their guidance in fieldwork. The structural data were plotted on stereographic projections using the GEOrient and GEOCalculator programs kindly made available for academic use by Dr Rod Holcombe (https://www.holcombe.net.au/software/georient.html). Comments from thesis examiners Professor Hugh Davies and Professor Ir. Benyamin Sapiie have enabled improvements to the final manuscript and are gratefully acknowledged.

References

Atmawinata, S., Hakim, A.S., and Pieters, P.E., 1989. *Geological Map of the Ransiki Sheet, Irian Jaya*. Geological Research and Development Centre, Bandung.

Babault, J., Viaplana-Muzas, M., Legrand, X., Driessche, J. van Den, González-Quijano, M., and Mudd, S.M., 2018. Source-to-sink constraints on tectonic and sedimentary evolution of the western Central Range and Cenderawasih Bay (Indonesia). *Journal of Asian Earth Sciences*, 156, p.265-287. DOI: 10.1016/j.jseaes.2018.02.004.

Bailly, V., Pubellier, M., Ringenbach, J.C., De Sigoyer, J., and Sapin, F., 2009. Deformation zone 'jumps' in a young convergent setting; the Lengguru fold-and-thrust belt, New Guinea Island. *Lithos,* 113 (1), p.306-317. DOI: 10.1016/j.lithos.2009.08.013.

Baldwin, S.L., Fitzgerald, P.G., and Webb, L.E., 2012. Tectonics of the New Guinea region. *Annual Review of Earth and Planetary Sciences, 40*, p.495-520. DOI: 10.1146/annurev-earth-040809-152540.

Cawood, P.A., 2005. Terra Australis Orogen: Rodinia breakup and development of the Pacific and Iapetus margins of Gondwana during the Neoproterozoic and Paleozoic. *Earth-Science Reviews*, 69, p.249-279. DOI:10.1016/j.earscirev.2004.09.001.

Charlton, T.R., 2000. Tertiary evolution of the Eastern Indonesia Collision Complex. *Journal of Asian Earth Sciences,* 18 (5), p.603-631. DOI: 10.1016/S1367-9120(99)00049-8.

Charlton, T.R., 2010. The Pliocene-Recent Anticlockwise Rotation of the Bird's Head, the Opening of the Aru Trough–Cendrawasih Bay Sphenochasm, and the Closure of the Banda Double Arc. *Proceedings, Indonesian Petroleum Association. 34th Annual Convention and Exhibition*.

Cloos, M., Sapiie, B., Ufford, A.Q. van, Weiland, R.J., Warren, P.Q., and McMahon, T.P., 2005. Collisional delamination in New Guinea: The geotectonics of subducting slab breakoff. *Geological Society of America Special Papers,* 400, p.1-51. DOI: 10.1130/2005.2400.

Crowhurst, P.V., Maas, R., Hill, K.C., Foster, D.A., and Fanning, C.M., 2004. Isotopic constraints on crustal architecture and Permo-Triassic tectonics in New Guinea: possible links with eastern Australia. *Australian Jour-*

nal of Earth Sciences, 51 (1), p.107-122. DOI: 10.1046/j.1400-0952.2003.01046.x.

Davies, H.J., 2012. The geology of New Guinea – the cordilleran margin of the Australian continent. *Episodes,* 35, p.87-102.

Decker, J., Bergman, S.C., Teas, P.A., Baillie, P., and Orange, D.L., 2009. Constraints on the tectonic evolution of the Bird's Head, West Papua, Indonesia. *Proceedings, Indonesian Petroleum Association. 33rd Annual Convention and Exhibition*.

Decker, J., Ferdian, F., Morton, A., Fanning, M., and White, L.T., 2017. New Geochronology Data from Eastern Indonesia – An Aid to Understanding Sedimentary Provenance in a Frontier. *Proceedings, Indonesian Petroleum Association, 41st Annual Convention*, IPA41-G-551, p.1-18. DOI: 10.29118/IPA.50.17.551.G.

Dow, D. and Sukamto, R., 1984. Western Irian Jaya: the end-product of oblique plate convergence in the late Tertiary. *Tectonophysics,* 106 (1), p.109-139. DOI: 10.1016/0040-1951(86)90053-3.

Fergusson, C.L., 1991. Thin-skinned thrusting in the northern New England Orogen, central Queensland, Australia. *Tectonics*, 10, p.797-806. DOI:10.1029/90TC02708.

François, C., Sigoyer, J. de, Pubellier, M., Bailly, V., Cocherie, A., and Ringenbach, J.C., 2016. Short-lived subduction and exhumation in Western Papua (Wandamen Peninsula): Co-existence of HP and HT metamorphic rocks in a young geodynamic setting. *Lithos,* 266-267, p.4–63. DOI: 10.1016/j.lithos.2016.09.030.

Gold, D.P., White, L.T., Gunawan, I., and Bou-Dagher-Fadel, M.D., 2017. Relative sea-level change in western New Guinea recorded by regional biostratigraphic data. *Marine and Petroleum Geology*, 86, p.1133-1158. DOI: 10.1016/j.marpetgeo.2017.07.016.

Gunawan, I., Hall, R., Augustsson, C., and Armstrong, R., 2014. Quartz from the Tipuma Formation, West Papua: New insights from geochronology and cathodoluminescence studies. *Proceedings, Indonesian Petroleum Association*, *38th Annual Convention and Exhibition*.

Gunawan, I., Hall, R., and Sevastjanova, I., 2012. Age, character and provenance of the Tipuma Formation, West Papua: new insights from detrital zircon dating. *Proceedings, Indonesia Petroleum Association*, *36th Annual Convention and Exhibition*.

Henderson, R.A., Donchak, P.J.T., and Withnall, I.W., 2013. Chapter 4 Mossman Orogen. *In*: Jell, P.A., (ed.), *Geology of Queensland,* Geological Survey of Queensland, p.225-304.

Hill, K.C. and Hall, R., 2003. Mesozoic-Cenozoic evolution of Australia's New Guinea margin in a west Pacific context. *In*: Hillis, R.R., and Müller, R.D. (eds.), *Evolution and Dynamics of the Australian Plate*. Geological Society of Australia Special Publication, 22, and Geological Society of America Special Paper, 372, p.265-290.

Irawan, D., 2015. *Karakteristik batuan induk Formasi Aiduna, Formasi Woniwogi, dan Formasi Piniya Cekungan Bintuni hubungannya dengan potensi hidrokarbon di daerah Ransiki dan sekitarnya. Kabupaten Manokwari Selatan, Provinsi Papua Barat*. *Unpublished* Master thesis, Padjadjaran University.

Irawan, D., Hamzah, A., Effendy, L.W., Hidayat, M.N., Sialagan, I.R., and Sutami, I., 2014. Studi potensi shale gas Cekungan Lengguru-Bintuni, Papua Barat. *Internal report*, Centre for Geological Survey, Geological Agency Indonesia, Bandung (Unpublished).

Jell, P.A. (ed.), 2013. *Geology of Queensland.* Geological Survey of Queensland, 970pp.

Jessop, K., Daczko, N.R., and Piazolo, S., 2019. Tectonic cycles of the New England Orogen, eastern Australia: A review. *Australian Journal of Earth Sciences,* 66 (4), p.459-496. DOI: 10.1080/08120099.2018.1548378.

Jost, B.M., Webb, M., and White, L.T., 2018. The Mesozoic and Palaeozoic granitoids of northwestern New Guinea. *Lithos*, 312-313, p.223-243. DOI: 10.1016/j.lithos.2018.04.027.

Jost, B.M., Webb, M., White, L.T., and Tiranda, H., 2021. Regional high-T/low-P metamorphism of the Kemum Basement High, Bird's Head, West Papua, Indonesia. *Journal of*

Metamorphic Geology, 39 (6), p.781-817. DOI: 10.1111/jmg.12586.

Kusnida, D., Albab, A., Nainggolan, T.B., and Firdaus, Y., 2023, The Occurrence of Recent-Subrecent Seabed Acoustic Anomalies and Its Relationship with Structural Uplift around the Waipoga Trough, West Papua-Indonesia. *Indonesian Journal on Geoscience*, 10 (1), p.109-117. DOI: 10.17014/ijog.10.1.109-117

Panggabean, H. and Pigram, C.J., 1989. *Geological Map of the Waghette Sheet, Irian Jaya*. Geological Research and Development Centre, Bandung.

Pieters, P.E., Hakim, A.S., and Atmawinata, S., 1985. *Geological Data Record Ransiki, Irian Jaya (2914-3014) Scale 1:250 000*. Irian Jaya Geological Mapping Project, GRDC Indonesia and BMR Australia.

Pieters, P., Pigram, C., Trail, D., Dow, D., Ratman, N., and Sukamto, R., 1983a. The stratigraphy of western Irian Jaya. *Proceedings, Indonesian Petroleum Association. 12th Annual Convention Jakarta*, p. 229-261.

Pieters, P.E., Pigram, C.J., Trail, D.S., Dow, D.B., Ratman, N., and Sukamto, R., 1983b. The Stratigraphy of Western Irian Jaya. *Bulletin Geological Research and Development Centre, Bandung*, p.14-48.

Pigram, C.J., and Sukanta, U., 1982. *Geological data record Taminabuan 1:250,000 sheet area Irian Jaya*. Geological Research and Development Centre, Bandung.

Pluijm, B.A. van der and Marshak, S., 2004. *Earth Structure: An Introduction to Structural Geology and Tectonics.* Second Edition. W. W. Norton & Company, New York, 672pp.

Ratman, N., Robinson, G.P., and Pieters, P.E., 1989. *Geological Map of the Manokwari Sheet, Irian Jaya*, 1: 250.000. Geological Research and Development Centre, Bandung.

Rosenbaum, G., 2018. The Tasmanides: Phanerozoic tectonic evolution of eastern Australia. *Annual Review of Earth and Planetary Sciences*, 46, p.291-325. DOI: 10.1146/annurev-earth-082517-010146.

Sapiie, B., Adyagharini, A.C., and Teas, P., 2010. New insight of tectonic evolution of Cendrawasih Bay and its implication for hydrocarbon prospect, Papua, Indonesia. *Proceedings, Indonesian Petroleum Association*, *34th Annual Convention and Exhibition.*

Saputra, S.E.A., 2021. *Cenozoic deformation and tectonics of eastern Bird's Head Peninsula, West Papua, Indonesia*. Unpublished *Ph.D thesis*, University of Wollongong. https://ro.uow.edu.au/theses1/1308/.

Saputra, S.E.A., Fergusson, C.L., Dosseto, A., Doherty, A., and Murray-Wallace, C.V., 2022. Late Quaternary neotectonics in the Bird's Head Peninsula (West Papua), Indonesia: implications for plate motions in northwestern New Guinea, western Pacific. *Journal of Asian Earth Sciences*, 236, 105336. DOI:10.1016/j.jseaes.2022.105336.

Sukanta, U. and Pigram, C.J., 1989. *Geological map of the Taminabuan Sheet, Irian Jaya, 1:250 000*. Geological Research and Development Centre, Bandung.

Thery, J.M., Pubellier, M., Thery, B., Butterlin, J., Blondeau, A., and Adams, C., 1999. Importance of active tectonics during karst formation. A Middle Eocene to Pleistocene example of the Lina Moutains (Irian Jaya, Indonesia). *Geodinamica Acta,* 12 (3-4), p.213-221. DOI: 10.1080/09853111.1999.11105344.

Torsvik, T.H., and Cocks, L.R.M., 2013. Gondwana from top to base in space and time. *Gondwana Research*, 24 (3-4), p. 999-1030. DOI:10.1016/j.gr.2013.06.012.

Visser, W.A. and Hermes, J.J., 1962. *Geological results of the exploration for oil in Netherlands New Guinea.* Koninklijk Nederlands Geologisch Mijnbouwkundig Genootschap, *Geologische Serie* 20, Staatsdrukkerij- en Uitgeverijbedrijf, 's-Gravenhage, 265pp.

Webb, M. and White, L.T., 2016. Age and nature of Triassic magmatism in the Netoni Intrusive Complex, West Papua, Indonesia. *Journal of Asian Earth Sciences*, 132, p.58-74. DOI: 10.1016/j.jseaes.2016.09.019.

Webb, M., White, L.T., Jost, B.M., Tiranda, H., and BouDagher-Fadel, M., 2020. The history of Cenozoic magmatism and collision in NW New Guinea–New insights into the tectonic

evolution of the northernmost margin of the Australian Plate. *Gondwana Research*, 82, p.12–38. DOI: 10.1016/j.gr.2019.12.010.

White, L.T., Hall, R., Gunawan, I., and Kohn, B., 2019. Tectonic mode switches recorded at the northern edge of the Australian Plate during the Pliocene and Pleistocene. *Tectonics,* 38 (1), p.281-306. DOI: 10.1029/2018TC005177.

Wyck, N. van and Williams, I.S., 2002. Age and provenance of basement metasediments from the Kubor and Bena Bena Blocks, central Highlands, Papua New Guinea: constraints on the tectonic evolution of the northern Australian cratonic margin. *Australian Journal of Earth Sciences*, 49 (3), p.565-577. DOI: 10.1046/j.1440-0952.2002.00938.x.